ARCHIVES of FOUNDRY ENGINEERING

ISSN (1897-3310)
Volume 2020
Issue 1/2020

95 – 104

16/1

Published quarterly as the organ of the Foundry Commission of the Polish Academy of Sciences

Consecutive Casting of Iron Bimetal with Low-Carbon Steel Interface Plate

W. Purwadi, B. Bandanadjaja, D. Idamayanti *, N. Lilansa
Politeknik Manufaktur Bandung
JI. Kanayakan no. 21 Dango, Bandung, Indonesia
* Corresponding author. E-mail address: idamayanti79@gmail.com

Received 11.09.2019; accepted in revised form 13.12.2019

Abstract

Consecutive casting of bimetallic applies consecutive sequences of pouring of two materials into a sand mold. The outer ring is made of NiHard1, whereas the inner ring is made of nodular cast iron. To enable a consecutive sequence of pouring, an interface plate made of low carbon steel was inserted into the mold and separated the two cavities. After pouring the inner material at the predetermined temperature and the interface had reached the desired temperature, the NiHard1 liquid was then poured immediately into the mold. This study determines the pouring temperature of nodular cast iron and the temperature of the interface plate at which the pouring of white cast iron into the mold should be done. Flushing the interface plate for 2 seconds by flowing nodular cast iron liquid as inner material generated a diffusion bonding between the inner ring and interface plate at pouring temperatures of 1350 °C, 1380 °C, and 1410 °C. The interface was heated up to a maximum temperature of 1242 °C, 1260 °C, and 1280 °C respectively. The subsequent pouring of white cast iron into the mold to form the outer ring at the interface temperature of 1000 °C did not produce a sufficient diffusion bonding. Pouring the outer ring at the temperature of 1430°C and at the interface plate temperature of 1125 °C produced a sufficient diffusion bonding. The presence of Fe3O2 oxide on the outer surface of the interface material immediately after the interface was heated above 900 ºC has been identified. Good metallurgical bonding was achieved by pouring the inner ring at the temperature of 1380°C, interface temperature of 1125 °C and then followed by pouring of the outer ring at 1430ºC and flushing time of 7 seconds.

Keywords: Consecutive casting, Bimetal, White cast iron, Interface plate, Casting temperature

1. Introduction

Casting product requires, in some cases, a combination of special properties such as abrasion resistance, corrosion resistance, high shock resistance, and good machinability. These properties are contradictory for a single material. The hardness is mostly contrary to the impact of resistance and machinability. For a particular application, the requirements of high-performance properties are only for the working surface of cast objects (Wróbel, Cholewa, & Tenerowicz, 2011). Bimetallic Casting is a method of combining two metallic materials with different properties by means of the casting process. The diffusion bonding in bimetallic casting is influenced by pressure, contact surface cleanliness, contact time, and contact temperature (Kumar, Krishnamoorthi, Ravisankar, & Angelo, 2009). The contact temperature in the diffusion process is at the rate of 50%-80% of the lowest material melting point (Li et al., 2018). In the previous study (Avcı, İlkay a, Şimşir, & Akdemir, 2009), the Grinding Roll prototype was made using the gravity casting method. A die blank of nodular cast iron was inserted into the mold, and the liquid white cast iron was then subsequently poured. Inserting an interface plate between the inner and outer material enables pouring of the inner and outer material in a sequence into the same mold. However, the interface plate served as a die blank as well, and the optimum temperature was set up in order to avoid initiation of cracks and produce a metallurgical bonding. The

preheating of the interface plate as a consequence of the first pouring created a good condition for a diffusion bonding between the interface plate and the subsequently poured outer ring material.

The volume ratios of liquid to solid affect significantly the interfacial microstructure. To achieve a sound interfacial microstructure a liquid–solid volume ratio of 10:1 and 12:1 is required (Xiong, Cai, & Lu, 2011). This ratio was then referred as the minimum ratio in designing the interface plate. An epitaxial interfacial layer of austenite can be precipitated onto the steel substrate from the liquid phase, and that the thickness of the layer can be controlled by soak time at 1250 °C (Lucey et al., 2012). In this study the soak temperature was set lower but the soaking time is longer due to higher mass provided by the inner ring. This study is aimed to produce a bimetallic casting of nodular cast iron-NiHard1 by applying an interface plate and pouring both of the materials in a sequence into the same mold.

2. Materials and Method

Bimetallic casting consists of the inner ring made of nodular cast iron and an outer ring made of NiHard1 white cast iron. Mold made of resin sand were used to form the casting. Two cavities in the mold were separated by a carbon steel interface plate. It was inserted into the mold prior to the pouring of liquid. A gating system was designed to enable the pouring of both materials in a certain sequence. Flow off tanks were designed to ensure the filling time of the cavity so that the interface temperature could be assured.

Figure 1 describes the gating system, flow off tanks and the interface plate. Two middle frequency induction furnaces were used to melt the two materials separately at the same time. First, the nodular cast iron liquid was poured into the mold to form the inner ring. After the interface plate gained the desired temperature, which was measured by placing a contact thermocouple in the bottom position of the interface plate, the NiHard1 liquid was then poured into the mold to form the outer ring.

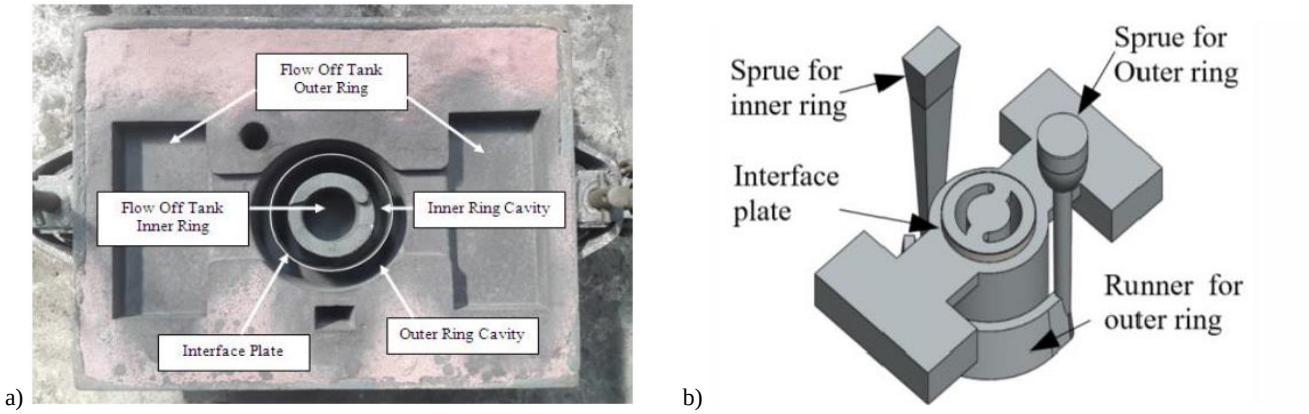

Fig. 1. Mold drag (a) and gating system and flow off tanks (b)

Table 1.
The chemical composition of the material

Material	Elements in Wt%								
	C	Si	Mn	Cr	Ni	Mo	P	S	other
Nodular CI	3.41	2.62	0.30						Mg 0.023
NiHard1	3.19	0.50	0.58	2.11	3.32	0.02	0.047	0.026	
Interface plate	0.12	0.03	0.56						

2.1. Material

This research was performed for two types of cast iron, nodular cast iron as the inner ring material and white cast iron (NiHard1) for the outer ring material. Low carbon steel was used as the material for the interface plate. The chemical composition was tested for each material by Optical Emission Spectrometry using ARL 3460.

Table 1 describes the elemental composition of materials as average value. The inner ring had an outer diameter of 147 mm, an inner diameter of 106 mm and a height of 120. The outer ring had an outer diameter of 188.45 mm, an inner diameter of 149.95 mm and a height of 100 mm.

2.2. Interface Temperature

To produce a diffusion bonding on the interface, the interface temperature at the time of pouring must have been in the range of 50%-80% of the lowest liquid-material point (Li et al., 2018). Pretrials by pouring liquid nodular cast iron at 1410°C into the mold caused a partial melting of the interface plate. Based on this, the pouring temperature of 1410°C was set as the maximum pouring temperature for the nodular cast iron. Pre-trials by

pouring Nihard1 liquid directly to die blank of low carbon steel plate have also been conducted to set the reference for determining the interface temperature. It was found that the die blank temperature of 1150 °C and pouring temperature of 1430 °C produced a diffusion bonding between poured Nihard1 and the die blank.

The interface temperatures were then set up slightly below 1150°C. To achieve the determined interface temperature, the cavity for the inner ring was added with a flow off tank, so that the nodular cast iron had enough time to raise the interface temperature up to slightly above the determined interface temperature. Pouring of the outer ring was done immediately after cooling process and the interface plate was at the correct temperature. A SolidCAST simulation was used to design the flow off tank. Figure 2 shows the flow off tank and the simulation. Interface temperature is considered as preheating temperature and this is related to crack.

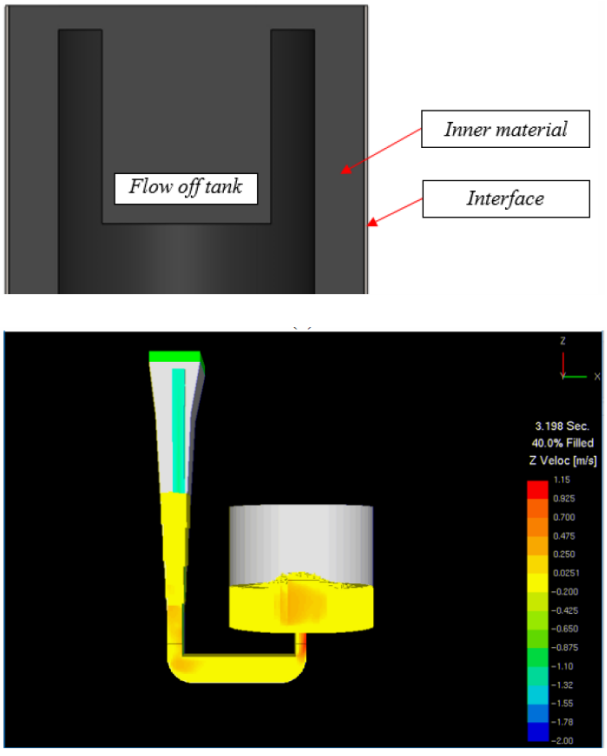

Fig. 2. Schematic of flow-off tanks as initial heater interfaces (a) and SolidCAST simulation (b)

Crack is to be avoided, and the susceptibility of steel to cold cracking is expressed as equation (1 and 2) below (Yurioka & Suzuki, 1983; Yurioka, Suzuki, Ohshita, & Saito, 1983) :

$$CE = C + A(C)\left\{\frac{Si}{24} + \frac{Mn}{6} + \frac{Cu}{15} + \frac{Ni}{20} + \frac{Cr+Mo+Nb+V}{5} + 5B\right\} \quad (1)$$

Whereas,

$$A(C) = 0.75 + 0.25\tanh\{20(C - 12)\} \quad (2)$$

A cracking index (Cl) is used to evaluate the probability of cold cracking and is expressed as equation (3)

$$CI = CE + 0.15\log H_{JIS} + 0.3\log(0.017 k_t \sigma_w) \quad (3)$$

The required preheating temperatures to avoid cold cracking is then determined by the following criterion $t_{100} \leq (t_{100})_{Cr}$ where t_{100} is the cooling time to 100 °C (212 °F). Critical time $(t_{100})_{Cr}$ is given as equation (4):

$$(t_{100})_{Cr} = \exp(67.6CI^3 - 182CI^2 + 163.8GI - 41) \quad (4)$$

2.3. Contact Pressure

Pressure at the contact area between the interface plate and casting material was necessary to facilitate a bonding and avoid any gap. The interface plate expanded during the heating process, which was caused by the direct contact to the inner ring liquid. During the following cooling process, the interface plate and the inner ring experienced a contraction. Since the coefficient of thermal expansion of low carbon steel is higher than those of nodular cast iron, the interface plate achieved higher contraction and this led further to a buildup of pressure at the contact area. Table 2 shows the coefficient of thermal expansion of nodular cast iron, low carbon steel and NiHard1.

Table 2.
The coefficient of material thermal expansion

No	Material	Coefficient of thermal expansion at 700°C (m m^{-1} $°C^{-1}$)
1	Nodular Cast Iron	13.8 (Davis, Mills, & Lampman, 1990)
2	Low-Carbon Steel	14.8 (Davis, Mills, & Lampman, 1990)
3	Ni-Hard 1	12.8 (Laird, Gundlach, & Rohrig, 2000)

Contraction and expansion of material can be expressed as follows:

$$\Delta L = L_0 C \Delta T \quad (5)$$

$$L_1 = L_0 + \Delta L \quad (6)$$

Where: ΔL = Change in diameter (m)
L_0 = Diameter at low temperature (m)
L_1 = Diameter at high temperature (m)
C = Thermal expansion coefficient (m m-1 ºC-1)

Dimensional changes at high temperatures and room temperatures are shown in Table 3. It can be identified that there was a slight difference in dimension between the two contact areas. The inner diameter of outer ring was smaller than the outer diameter of the interface, which indicated a contact pressure between the interface plate and the outer ring. Since the inner diameter of the interface plate was smaller than the outer diameter of the inner ring, a contact pressure was generated between the interface plate and the outer ring.

Table 3.
Material diameter before and after expansion

Temperature (°C)	The diameter of the Inner Ring (mm)			The diameter of the Interface Ring (mm)			Diameter of Outer Ring (mm)		
	inner	center	outer	inner	center	outer	inner	center	outer
700	106	127.25	148.5	148.5	150	151.5	151.5	170.75	190
20	106	126.12	147.37	147	148.5	150	149.9	169.2	188.45

2.4. Contact Surface

A clean contact surface is a requisite for achieving diffusion bonding (Li et al., 2018). The interface plate was therefore cleaned from dirt and oxides prior to the assembly of the mold, and the interface plate was also rinsed with ethanol.
During the pouring of the inner ring and prior to the pouring of the outer ring, there was time available that may have facilitated a formation of dirt on the surface of the interface plate. By the flowing of the liquid (flushing) for several seconds by applying a flow off tank, dirt was removed. It is found that a flushing time of 7 seconds by the liquid temp erature of 1430°C was adequate to generate a sufficient bonding (Avcı et al., 2009). Figure 3 and Figure 4 describe the flushing process by the flowing of the liquid to the flow off tank for the inner ring and outer ring.

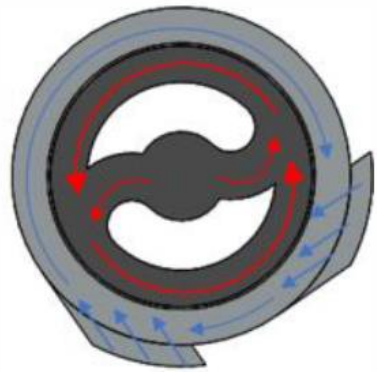

Fig. 3. Schematic of flushing material from the inlet for the inner ring

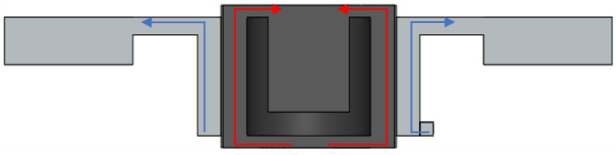

Fig. 4. Schematic of flushing the material towards the flow off tank

2.5. Contact Time

The contact time between the liquid and interface plate was needed to preheat the interface plate to facilitate a diffusion bonding. This was achieved by adding flow off tanks to the design as shown in Figure 5. The contact time in this study was set for two seconds for the inner material and seven seconds for the outer material.

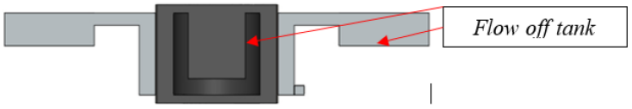

Fig. 5. Flow off tank

To minimize the turbulence during the filling process, a pressurized gating system was applied. Contact time was determined by calculating the velocity, volume of cavities, and cross-section area of ingate. This was then verified and simulated with the SolidCAST application (Figure 6).

a)

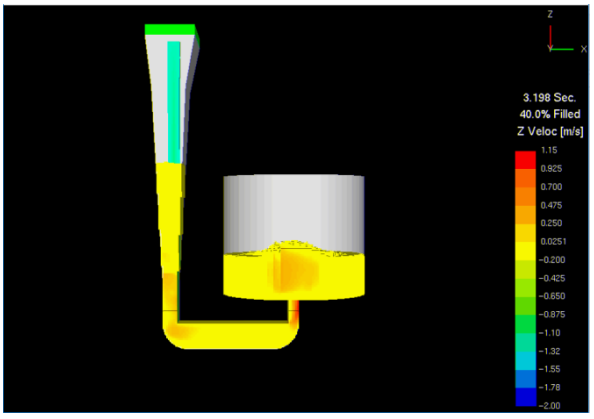

b)

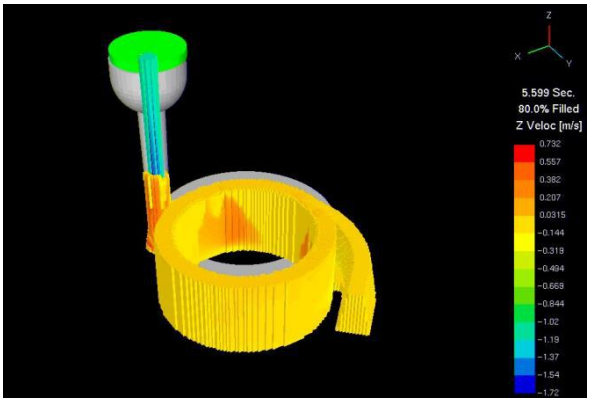

Fig. 6. The simulation of liquid flow of inner material (a) and outer material (b)

2.6. Casting Process

The inner ring was cast by pouring the liquid nodular cast iron at the pouring temperature of 1320 °C, 1350 °C, 1380 °C, and

1410 °C. The casting was then cooled until the interface plate reached the determined temp erature, which was set as 1000°C and 1125 °C.

Table 4.
Shows the trial parameters

Trial	Pouring Temperature of inner ring (^{o}C)	Temperature of interface plate (^{o}C)	Pouring Temperature of inner ring (^{o}C)
1	1320	1125	1430
2	1320	1000	1430
3	1350	1125	1430
4	1350	1000	1430
5	1380	1125	1430
6	1380	1000	1430
7	1410	1125	1430
8	1410	1000	1430

NiHard1 liquid was then immediately poured into the mold to form the outer ring at a constant temperature of 1430 °C. The increase of the interface plate temperature was measured with a thermocouple, which was placed in contact with it. Table 4 shows the trial parameters and three casting were made for each trial.

2.7. Microstructural observation and hardness testing

Testing of hardness was conducted by applying Vickers' micro hardness testing with a constant static load of.0.2 kg. Optical microscope (OLYMPUS GX 71) was used to observe the microstructure. EDS Testing (SEM HITACHI SU 3500 and EDAX) was carried out to identify the elemental composition on a micro area. Samples were etched with Nital 3%.

3. Results and discussion

3.1. Casting

Pouring the NiHard1 liquid for the outer ring at the interface temperature of the 1000 °C did not produce any bonding between the interface plate and the outer material, so the initial heating temperature range had to be increased to 80%-90% of the lowest liquid point. By pouring temperature of 1410 °C for the inner ring, the interface plate was partially melted so that the inner ring material entered the outer ring cavity. Samples were taken from the casting (Figure 7a) and testing was conducted on the cross section area (Figure 7b).

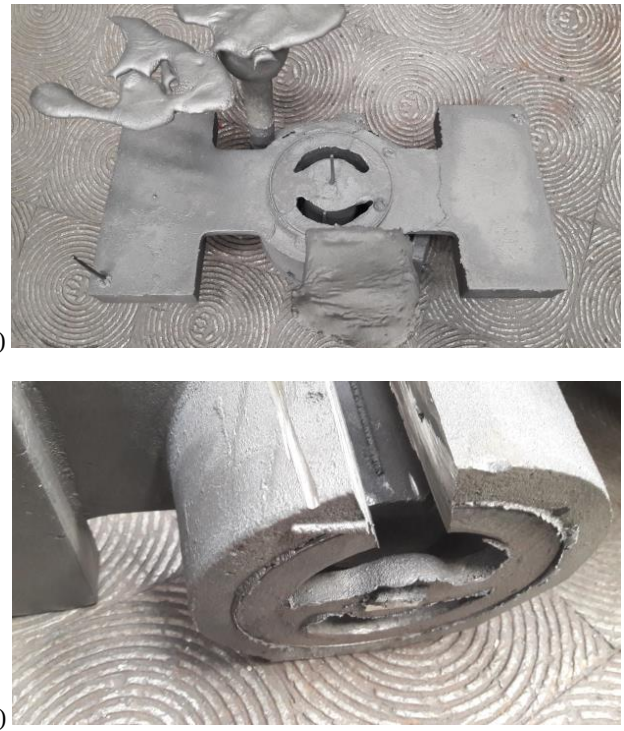

Fig. 7. Casting tree incl. Flow off tanks (a) and cut off position (b)

3.2. Temperatures

The temperature of the interface plate was monitored by using a data logger and thermocouple which was placed in contact with the interface plate. Directly after pouring the inner ring at diverse temperatures, a maximum temperature of the interface plate was achieved. Table 5 shows the pouring temperature of the inner ring and the maximum temperature of the interface plate. All of pouring temperatures resulted in an interface temperature above the targeted temperature (1125°C). However, the pouring temperature of the inner ring of 1320 °C and the maximum interface temperature of 1219 °C did not produce a bonding.

Table 5.
Pouring and maximum interface temperature

Pouring temperature of the inner ring (^{o}C)	Max. Interface Temperature (^{o}C)
1320	1219
1350	1242
1380	1260
1410	1280

3.3. Microstructures of Material

3.3.1 Pouring the inner ring at a temperature of 1320 ºC

By pouring the inner ring at 1320 °C, metallurgical bonding between the interface plate and the inner ring only occurred near to the ingate area. The micrographs in Figure 8 show the presence

of a gap at the contact area (a) and the microstructure on the inner ring (b) which consists of ferrite, pearlite and nodular graphite.

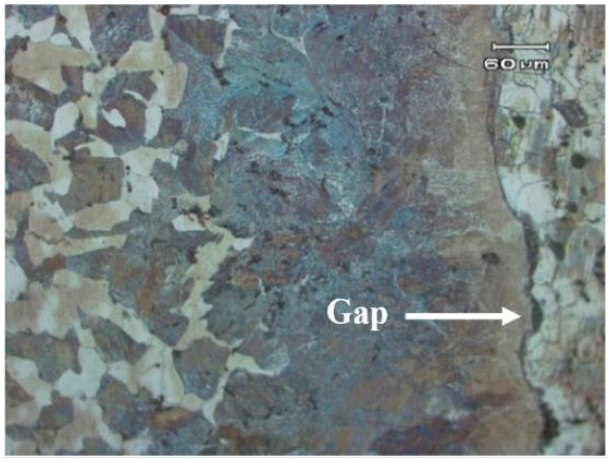

a)

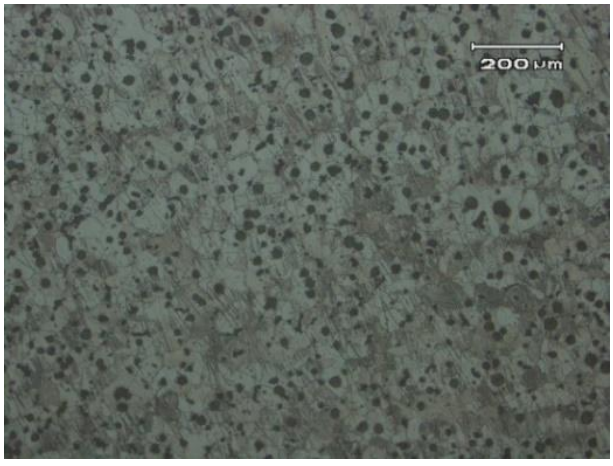

b)

Fig. 8. Micrograph by pouring temperature of 1320 ºC; (a) contact section (b) inner part. Etched with 3% Nital

3.3.2 Pouring the inner ring at a temperature of 1350 ºC

By pouring the inner ring at 1350 ºC, metallurgical bonding between the interface plate and the inner ring was achieved on the entire contact surface.

The micrograph in Figure 9 shows the presence of flake Graphite in some spots due to the considerably insufficient Mg treatment. Pearlite formed close to the contact area and cementite formed along the boundary of pearlite islands. The hardness value of pearlite was found to vary by the area/zone and its cooling rate, respectively.

By pouring the inner ring at 1350 ºC, metallurgical bonding between the interface plate and the inner ring was achieved on the entire contact surface. The presence of pearlite may indicate the higher content of carbon compared to the rest part of the interface plate. This additional content of carbon may have considerably come from the inner ring material. Table 6 shows the distribution of pearlite hardness which indicated difference in the carbon content in the pearlite for each area (Davis et al., 1990). The difference in carbon content was also an indication of carbon diffusion in the contact area between the inner material and the interface material (Avcı et al., 2009) and a diffusion bonding.

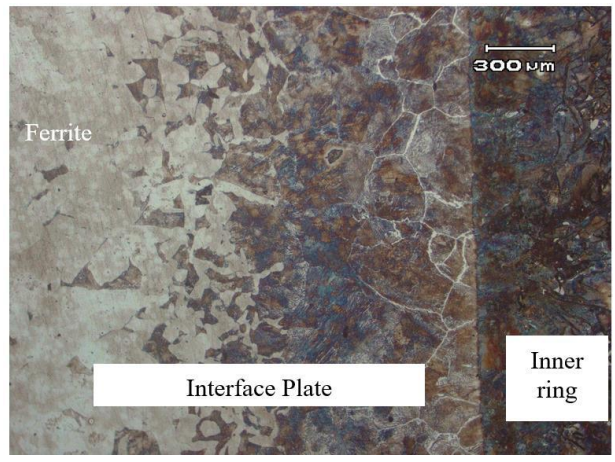

a)

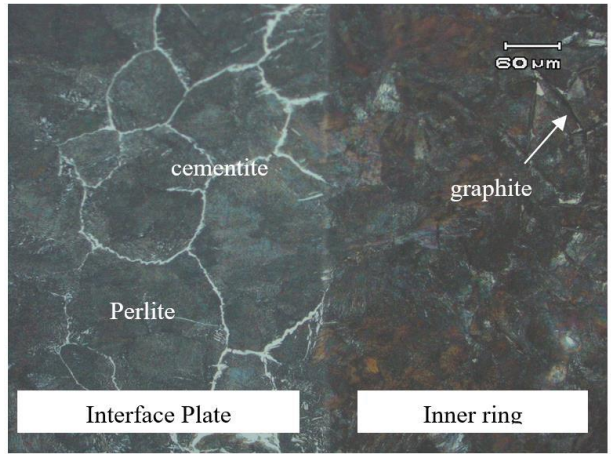

b)

Fig. 9. Micrographs of the contact area interface-inner ring by pouring temperature of 1350 ºC; (a) contact section; (b) inner parts. Etched with 3% Nital

Table 6.
Pearlite hardness in average values at some positions

Hardness (HV)	Interface	Contact area	Inner
	196.7	286.1	372.8

3.3.3 Pouring the inner ring at the temperature of 1380 °C

By pouring the inner ring at 1380 °C, the interface plate became softer and weaker so that pressure generated by the inner ring liquid might tear off the interface plate and the liquid subsequently entered the outer material cavity. The micrograph in Figure 10 shows the presence of nodular Graphite in the matrix of ferrite. Along the contact line to the interface plate, the microstructure of the inner ring is dominated by pearlite. Cementite formed along the boundary of pearlite islands and at the contact area. The hardness value of cementite at the interface is 499.8 HV. Table 7 shows the hardness value of pearlite at the interface plate and contact area. As can be seen in Figure10(b),

the liquid cast iron teared off some of the interface plate and flowed into the outer ring cavity.

Table 7.
Pearlite hardness values at p our temperature of 1380 °C

Hardness (HV)	Interface	Contact area	Inner
	233.1	338.7	–

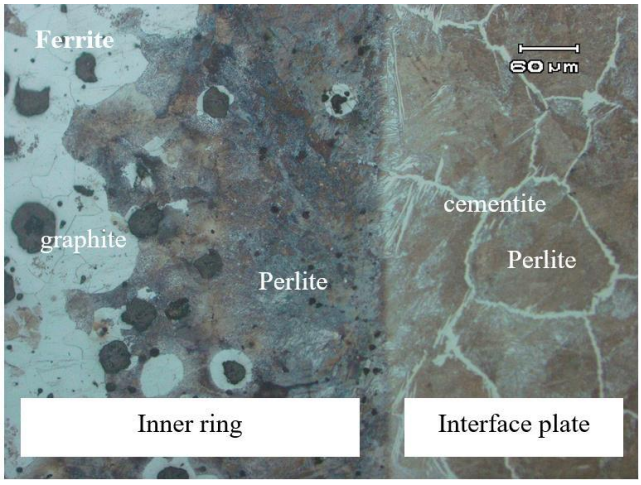

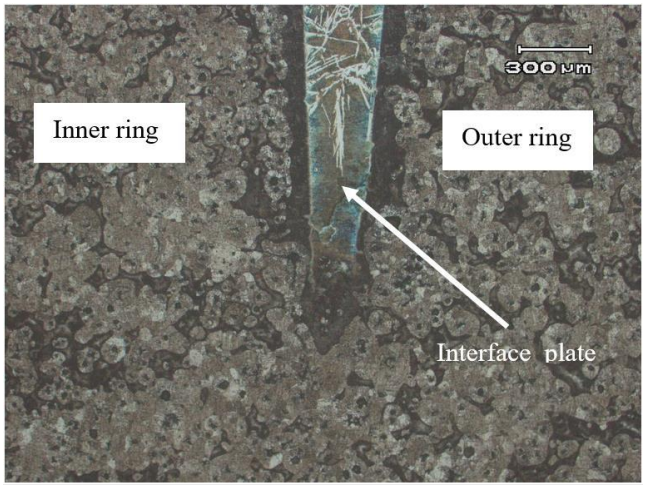

Fig. 10. micrograph by pouring temperature of 1380 ° C; (a) interface area; (b) interface plate. Etched with 3% Nital

3.3.4 Pouring the inner ring at the temperature of 1410 °C

Pouring the inner ring at the temperature of 1410°C raised the temperature of the interface plate enormously, so that the interface plate heated up to 1280°C. The interface p late became soft and tore off at some spots. The inner ring material flowed through these spots into the outer ring cavity. This material came to direct contact with the NiHard1 liquid by subsequent pouring of the outer ring. Figure 11 shows the microstructure of the contact area which consists of martensite and M3C Carbide in the NiHard1 area, pearlite and cementite in the rest interface plate and nodular graphite in the inner ring material.

Table 8.
Value of phase hardness at pouring temperature 1410 °C

Section	Hardness (HV 0.2)
Perlite on interface	321.1
Martensite in the contact area	504
M_3C on NiHard 1	985
Martensi t e on NiHard1	607.8

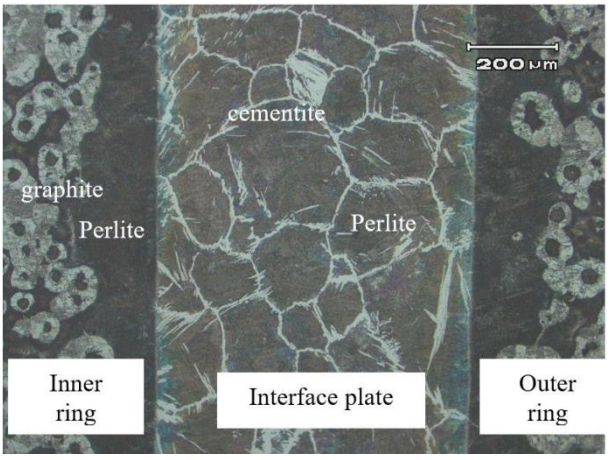

a)

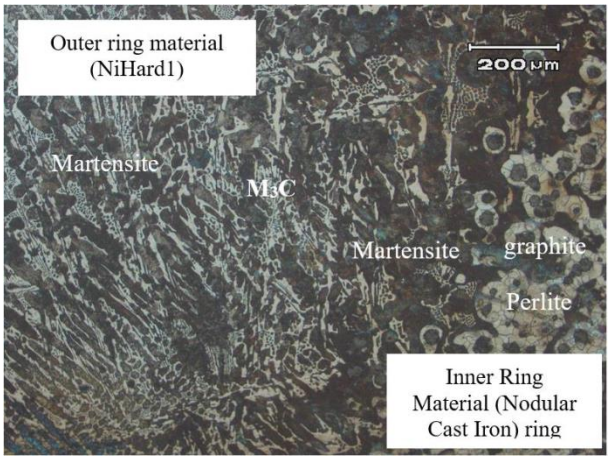

b)

Fig. 11. Micrographs by pouring the inner ring at temperature 1410 °C; (a) nodular cast iron in outer and inner ring cavities; (b) direct contact inner and outer ring material . Etched with Nital 3%.

The hardness values of each phase are listed in Table 8. There were differences in martensite hardness in the contact area and martensite on the NiHard1 base material, which was considerably determined by the concentration of carbon in martensite in both regions.

3.3.5 Subsequent pouring of the outer ring at the interface temperature of 1000 πC

Nihard1 liquid was poured at the pouring temperature of 1430°C into the mold immediately after the interface p late reached the temperature of 1000°C (shown in the Table 4 as trial 2, 4, 6 and 8). Macro and microstructural observations have been conducted to the casting product. As shown in Figure 11, there

was no bonding achieved by pouring the outer ring material at this interface temperature. It can be therefore concluded that the interface temperature of 1000 ºC is inadequate to produce a diffusion bonding.

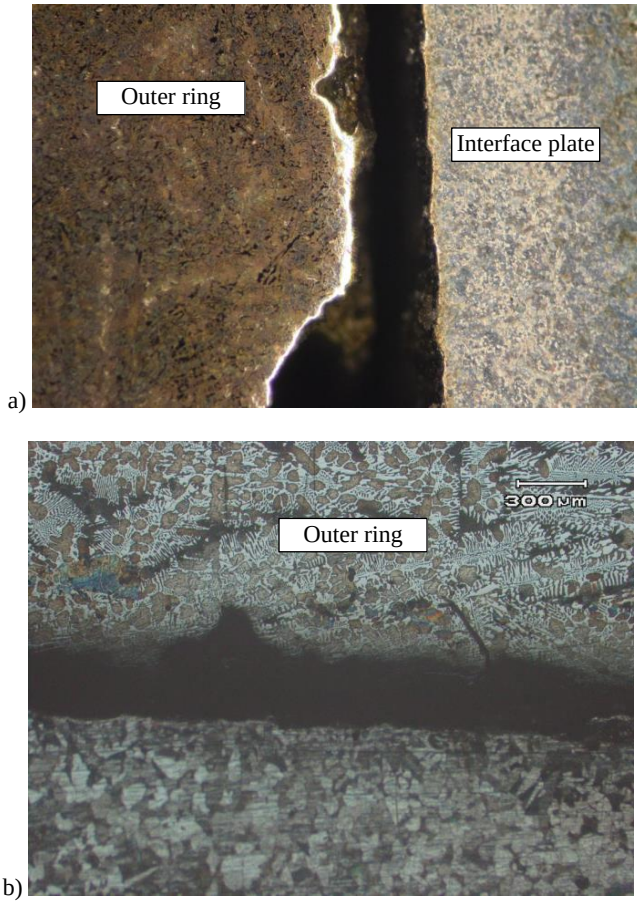

a)

b)

Fig. 12. Micrograph by 1000 ºC interface temperature; (a) gap between interface and the outer ring; (b) the closest contact area of the outer part to the interface plate

Since there was no achieved bonding between the material and the interface plate, it can be concluded that the interface temperature of 1000 ºC was inadequate to produce a diffusion bonding.

3.3.6 Subsequent pouring of the outer ring at the interface temperature of 1125ºC

Pouring the inner ring at 1320 °C and followed by pouring the outer ring at 1430°C at the interface temperature of 1125 °C (90% of the lowest melting temperature) as shown in Table 4 as trial 1 did not produce a metallurgical bonding of the outer ring to the interface plate. Bonding between the interface and the outer material did not occur at all. Metallurgical bonding between inner material and outer material was not identified. Gap was found at almost along the contact line between the interface plate and inner material (Figure 8a). Pouring the inner ring at 1350 °C and followed by pouring the outer ring at 1430°C at the interface temperature of 1125 °C as shown in the Table 4 as trial 3 did not produce a metallurgical bonding of the outer ring to the interface plate, whereas an excellent bonding of interface plate to the inner ring was obtained (Figure 12a). Bonding between the interface and the outer material did not occur at the entire contact surface. Figure 13 shows the microstructure at the contact area between the outer ring and interface plate. The NiHard1 area (outer ring) consisted predominantly of martensite and M_3C carbide.

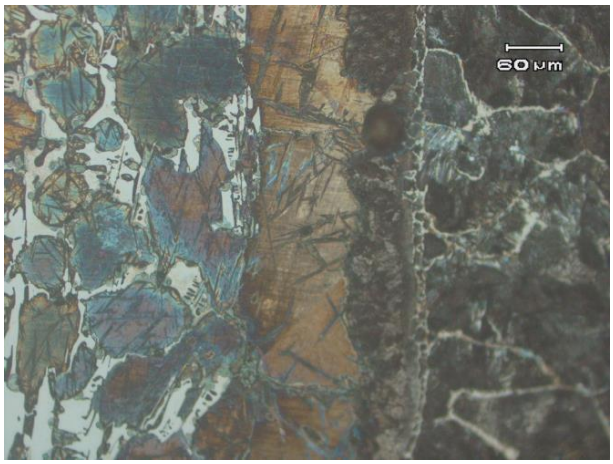

Fig. 13. Micrograph of contact area as resulted from pouring temperature of 1430°C, interface temperature of 1125ºC and pouring temperature of the inner ring at 1350°C

The appearance of iron oxide at the pouring time interval of inner material and outer material prevented flawless contact at the interface and the bonding respectively.

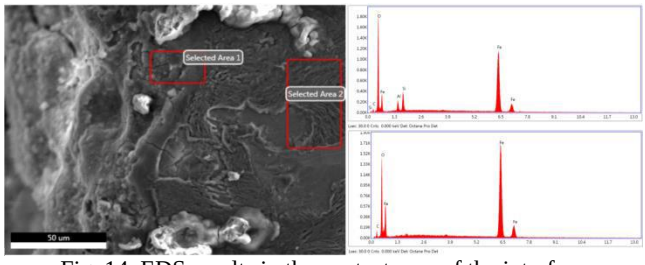

Fig. 14. EDS results in the contact area of the interface

Iron oxide formed due to the reaction between iron and oxygen or iron with water vapor. The appearance of oxide on the interface is proven by the EDS test results as shown in Figure 14. The EDS results show the high oxygen values found in the contact area interface with the outer material. This oxygen is present in the form of iron oxide. Referring to the Ellingham diagram, it is found that the reaction of Fe and O with the lowest Gibs energy is the reaction for the formation of Fe_2O_3.

Pouring the inner ring at 1380 °C and followed by pouring the outer ring at 1430°C at the interface temperature of 1125 °C as shown in the Table 4 as trial 5 generated metallurgical bonding between the interface plate and the outer ring. Bonding between the interface plate and the inner material also occurred at the entire contact surface of both materials. The contact area at the interface plate became softer. In addition to this, the flushing time of 7 seconds pushed the oxide upwards and rinsed the contact

surface. Flushing time is the time needed for the liquid to pass through the cavity of the outer ring to the flow off tank. Figure 15 shows that at the contact area, the pearlite grain became very fine and was surrounded by cementite at the grain boundary. Pearlite in other areas in the interface plate remained coarse. The microstructure of NiHard1 material close to the contact area was predominantly martensite.

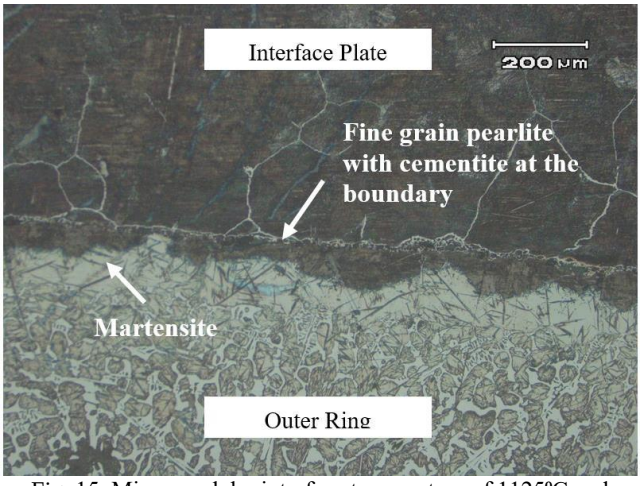

Fig. 15. Micrograph by interface temperature of 1125ºC and pouring temperature of the inner ring of 1380°C (trial 5)

Pouring the inner ring at 1410 °C and followed by pouring the outer ring at 1430°C at the interface temp erature of 1125 °C as shown in the Table 4 as trial 7 did not produce a good bimetallic casting. The interface plate was torn off in some spots resulting in the inner ring material entering into the cavity of outer ring. Furthermore, this caused a direct contact to the inner ring material by subsequent pouring of the outer ring material (Figure 15).

3.4. Bonding Fraction

The diffusion bonding between the inner material and the interface plate occurred at pouring temperatures of 1350 °C, 1380 °C, and 1410 °C and the resulting highest interface temperatures of 1242 °C, 1260 °C, and 1280 °C, respectively (Table 5). At these temperatures, the bonding fraction varies from 78 to 100%. In some spots, gaps and porosities at the contact area have been identified. By pouring the inner ring liquid at the temperature of 1320 °C and the maximum interface temp erature of 1219 °C, diffusion bonding occured only in a small area in the inner ring close to the ingate area. The percentage fraction of bonding is described in Figure 16.

By pouring the outer material at the interface temperature of 1000°C, diffusion bonding was not performed. Higher interface temperature (1125°C) and pouring temperature of inner ring of 1350°C could not generate a bonding as well. By pouring the inner ring at the temperature of 1380°C, the interface temperature of 1125°C and subsequent pouring of outer ring at a temperature of 1430°C, diffusion bonding occurred almost in all area of the interface.

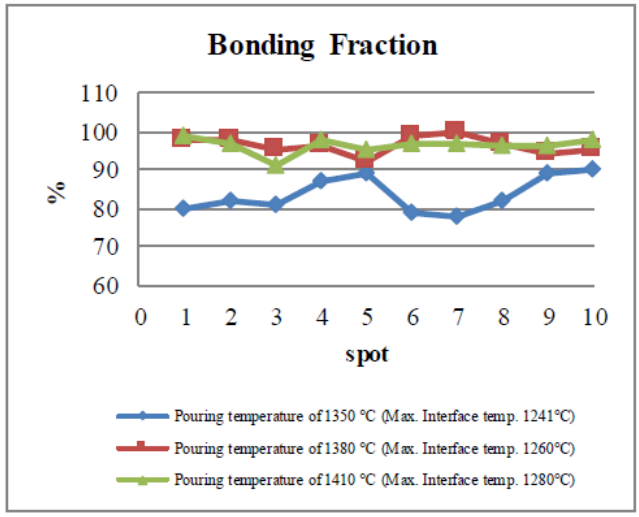

Fig. 16. The bonding fraction of the interface plate to the inner ring at various pouring temperature

4. Conclusions

Bimetallic products of nodular cast iron-white cast iron can be produced by consecutive casting, in which nodular cast iron as inner material is poured prior to the pouring of the outer material. An interface plate made of low carbon steel is inserted into the mold to separate inner and outer material. Good surface cleanliness, available contact pressure during solidification and cooling process, accurate pouring and interface temperatures, and adequate flushing time ensure the diffusion bonding. Since the available contact time between interface plate and base material by a casting process is very limited, the required interface temperature prior to the pouring of base material liquid for enabling diffusion bonding should be increased up to 90% of the lowest melting point. Flushing the interface plate by flowing liquid nodular cast iron for 2 seconds at pouring temperature of 1350 °C to 1410 °C created sufficient diffusion bonding between the inner ring and interface plate. The diffusion bonding may be hindered by the formation of iron oxide on the surface of the interface plate during the interval time between the first and second pouring. To form a metallic bonding between the interface plate and NiHard1 outer ring, an interface temperature of 1125°C, pouring temperature of 1430°C and flushing time of 7 seconds are to be applied.

Acknowledgments

The authors acknowledge to RISTEKDIKTI which funded this research as a part of HIBAH PUSN research grant. Authors also would thank to POLMAN Bandung an all colleagues for the support in all sector.

References

[1] Avcı, A., İlkaya, N., Şimşir, M., & Akdemir, A. (2009). Mechanical and microstructural properties of low-carbon steel-plate-reinforced gray cast iron. *Journal of Materials Processing Technology*. 209(3), 1410-1416.

[2] Davis, J.R., Mills, K.M., Lampman, S.R. (1990). *Metals handbook. Vol. 1. Properties and selection: irons, steels, and high-performance alloys*. ASM International, Materials Park, Ohio 44073, USA, 1990. 1063.

[3] Kumar, S.S., Krishnamoorthi, J., Ravisankar, B. Angelo, P. C. (2009). *Methodology to evaluate the quality of diffusion bonded joints by ultrasonic method*.

[4] Laird, G., Gundlach, R., Rohrig, K. (2000). *Abrasion-resistant cast iron handbook*. American Foundry Society Illinois.

[5] Li, Y., Gong, M., Wang, K., Li, P., Yang, X., & Tong, W. (2018). Diffusion behavior and mechanical properties of high chromium cast iron/low carbon steel bimetal. *Materials Science and Engineering.* A, 718, 260-266.

[6] Lucey, T., Wuhrer, R., Moran, K., Reid, M., Huggett, P., & Cortie, M. (2012). Interfacial reactions in white iron/steel composites. *Journal of Materials Processing Technology*. 212(11), 2349-2357. https://doi.org/10.1016/j.jmatprotec.2012.06.025.

[7] Wróbel, T., Cholewa, M., & Tenerowicz, S. (2011). Examp les of material solutions in bimetallic layered castings. *Archives of Foundry Engineering*. 11(3), 11-16.

[8] Xiong, B., Cai, C., & Lu, B. (2011). Effect of volume ratio of liquid to solid on the interfacial microstructure and mechanical properties of high chromium cast iron and medium carbon steel bimetal. *Journal of Alloys and Compounds*. 509(23), 6700-6704. https://doi.org/10.1016/j.jallcom.2011.03.142.

[9] Yurioka, N., Suzuki, H. (1983). *Determination of necessary preheating temperature in steel welding*.

[10] Yurioka, N., Suzuki, H., Ohshita, S., & Saito, S. (1983). Determination of Necessary Preheating Temperature in Steel Welding. *Welding Journal* (Miami, Fla), 62(6).

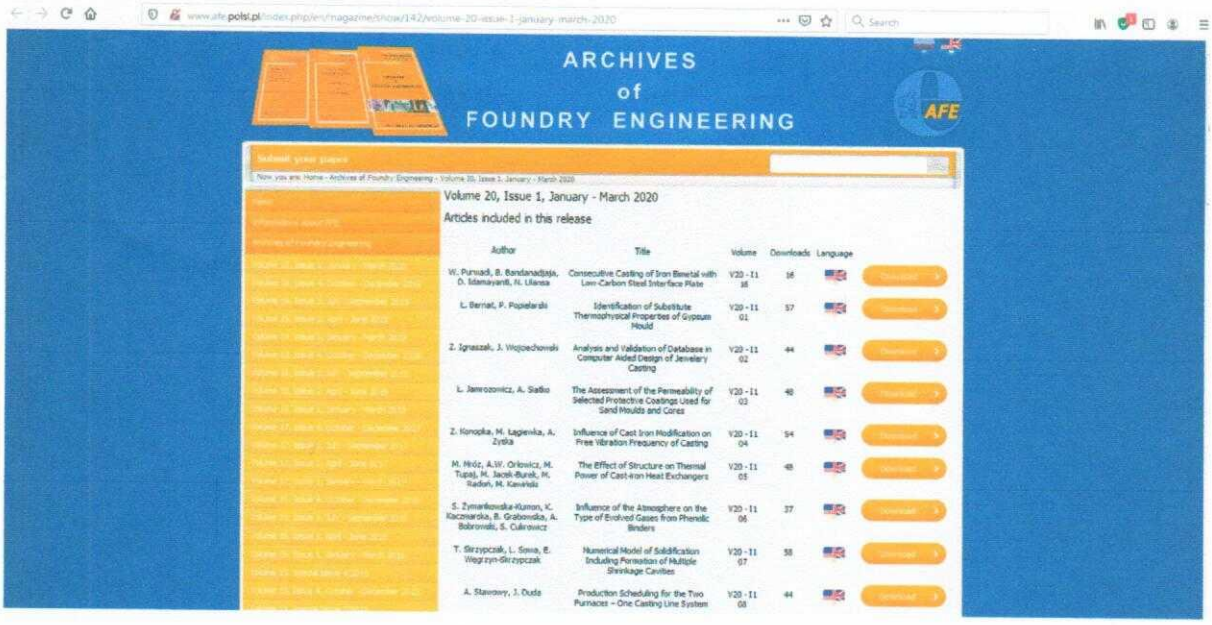
www.afe.polsl.pl/index.php/en/magazine/show/142/volume-20-issue-1-january-march-2020
ARCHIVES
of
FOUNDRY ENGINEERING
AFE
Volume 20, Issue 1, January - March 2020
Articles included in this release
Author
Title
Volume
Downloads
Language
W. Purnadi, B. Bandanadjaja, D. Idamayanti, N. Llansa
Consecutive Casting of Iron Bimetal with Low-Carbon Steel Interface Plate
V20 - I1 16
16
L. Bernat, P. Popielarski
Identification of Substitute Thermophysical Properties of Gypsum Mould
V20 - I1 01
57
Z. Ignaszak, J. Wojciechowski
Analysis and Validation of Database in Computer Aided Design of Jewelery Casting
V20 - I1 02
44
L. Jamrozowicz, A. Sadło
The Assessment of the Permeability of Selected Protective Coatings Used for Sand Moulds and Cores
V20 - I1 03
48
Z. Konopka, M. Łagiewka, A. Zyska
Influence of Cast Iron Modification on Free Vibration Frequency of Casting
V20 - I1 04
54
M. Nicz, A.W. Orłowicz, M. Tupaj, M. Jacek-Burek, H. Radoń, M. Kawiński
The Effect of Structure on Thermal Power of Cast-iron Heat Exchangers
V20 - I1 05
48
S. Żymankowska-Kumon, K. Kaczmarska, B. Grabowska, A. Bobrowski, S. Cukrowicz
Influence of the Atmosphere on the Type of Evolved Gases from Phenolic Binders
V20 - I1 06
37
T. Skrzypczak, L. Sowa, E. Węgrzyn-Skrzypczak
Numerical Model of Solidification Including Formation of Multiple Shrinkage Cavities
V20 - I1 07
58
A. Stawowy, J. Duda
Production Scheduling for the Two Furnaces – One Casting Line System
V20 - I1 08
44

Submit your paper

Volume 20, Issue 1, January - March 2020

Articles included in this release

Author	Title	Volume	Downloads	Language	
W. Purwadi, B. Bandanadjaja, D. Idamayanti, N. Lilansa	Consecutive Casting of Iron Bimetal with Low-Carbon Steel Interface Plate	V20 - I1 16	15		Download
Ł. Bernat, P. Popielarski	Identification of Substitute Thermophysical Properties of Gypsum Mould	V20 - I1 01	57		Download
Z. Ignaszak, J. Wojciechowski	Analysis and Validation of Database in Computer Aided Design of Jewelery Casting	V20 - I1 02	44		Download
Ł. Jamrozowicz, A. Siatko	The Assessment of the Permeability of Selected Protective Coatings Used for Sand Moulds and Cores	V20 - I1 03	48		Download
Z. Konopka, M. Łągiewka, A. Zyska	Influence of Cast Iron Modification on Free Vibration Frequency of Casting	V20 - I1 04	54		Download
M. Mróz, A.W. Orłowicz, M. Tupaj, M. Jacek-Burek, M. Radoń, M. Kawiński	The Effect of Structure on Thermal Power of Cast-iron Heat Exchangers	V20 - I1 05	48		Download
S. Żymankowska-Kumon, K. Kaczmarska, B. Grabowska, A. Bobrowski, S. Cukrowicz	Influence of the Atmosphere on the Type of Evolved Gases from Phenolic Binders	V20 - I1 06	37		Download
T. Skrzypczak, L. Sowa, E. Węgrzyn-Skrzypczak	Numerical Model of Solidification Including Formation of Multiple Shrinkage Cavities	V20 - I1 07	58		Download
A. Stawowy, J. Duda	Production Scheduling for the Two Furnaces – One Casting Line System	V20 - I1 08	44		Download
P. Szymański, K. Gawdzińska, D. Nagolska	Attempts to Prepare Precision Composite Castings by Sintering Al2O3/AlSi11 Using Underpressure	V20 - I1 09	54		Download
R. Sika, M. Rogalewicz, A. Kroma, Z. Ignaszak	Open Atlas of Defects as a Supporting Knowledge Base for Cast Iron Defects Analysis	V20 - I1 10	62		Download
Md. Sojib S. Hossain, A. K. M. Bazlur B. Rashid	Preconditiong and Inoculation of Low Sulphur Grey Iron	V20 - I1 11	41		Download
M. Stachowicz, Ł. Pałyga, D. Kępowicz	Influence of Automatic Core Shooting Parameters in Hot-Box Technology on the Strength of Sodium Silicate Olivine Moulding Sands	V20 - I1 12	37		Download
A. Kurzawa, D. Pyka, K. Jamroziak	Analysis of Ballistic Resistance of Composites with EN AW-7075 Matrix Reinforced with Al2O3 Particles	V20 - I1 13	47		Download
M. Matejka, D. Bolibruchova a, J. Kasińska b, M. Kuriš	Study of AlSi9Cu3 Alloy Crystallization Process with Increased Iron Content at Different Number of Remelts	V20 - I1 14	53		Download
Rong Li, Lunjun Chen, Qi Zeng, Ming Su, Zhiping Xie	Optimization of Al-Cu Cast Alloy Composition for Hydraulic Valves	V20 - I1 15	45		Download
Ł. Petrus, A. Bulanowski, J. Kolakowski, M. Brzeżański, M. Urbanowicz, J. Sobieraj, G. Matuszkiewicz, L. Szwalbe, K. Janerka	The Influence of Selected Melting Parameters on the Physical and Chemical Properties of Cast Iron	V20 - I1 17	11		Download
J. Kamińska, S. Puzio, M. Angrecki	Effect of Bentonite Clay Addition on the Thermal and Mechanical Properties of Conventional Moulding Sands	V20 - I1 18	3		Download
D. Martinec, R. Pastirčák, E. Kantoríková	Using of Technology Semisolid Squeeze Casting by Different Initial States of Material	V20 - I1 19	5		Download
P. Kaliuzhnyi	Influence of Sand Fluidization on Structure and Properties of Aluminum Lost Foam Casting	V20 - I1 20	5		Download

Find article

Phrase

Search

KAPITAŁ LUDZKI
NARODOWA STRATEGIA SPÓJNOŚCI

UNIA EUROPEJSKA
EUROPEJSKI
FUNDUSZ SPOŁECZNY

Man- the best investment!

Project co-funded by the European Union under the European Social Fund.

Archives of Foundry Engineering

Country	Poland - SIR Ranking of Poland
Subject Area and Category	Engineering Industrial and Manufacturing Engineering Materials Science Metals and Alloys
Publisher	Polish Academy of Sciences
Publication type	Journals
ISSN	18973310, 22992944
Coverage	2012-ongoing
Scope	Thematic scope includes scientific issues of foundry industry: Theoretical Aspects of Casting Processes, Innovative Foundry Technologies and Materials, Foundry Processes Computer Aiding, Mechanization, Automation and Robotics in Foundry, Transport Systems in Foundry, Castings Quality Management, Environmental Protection. Why subscribe and read

9

H Index